Design of a Swage Pin without Swage Ball for a Swaging Process in Hard Disk Drive using a Finite Element Method

Arbtip Dheeravongkit [*1], Sirawat Modmontin [*2], Anon Pichittanabodeekun [*3], Kittikorn Kemsuk [*4]

* *Institute of Field Robotics, King Mongkut's University of Technology Thonburi*
126 Pracha-u-tid road, Bangmod, Thrungkru, Bangkok, Thailand
[1]arbtip@fibo.kmutt.ac.th
[2]sirawat.mod@gmail.com
[3]anon.pichit@gmail.com
[4]gravity_broken@hotmail.com

***Abstract*— Ball swaging is a general method in head stack assembly process to permanently attach Head Gimbal Assemblies (HGAs) on the actuator arm. During the process, a swage pin guides a sequence of swage balls to move with desired velocity through the swage hole. These swage balls cause deformation on base plates of HGAs to tightly attach to the actuator arm. The common problem found in the process is the loose attachment between base plates and actuator arm. One possible cause of the problem is the oscillation of the swage pin during the process, which might result in the rotation and misalignment of the swage ball. According to this hypothesis, this research has studied the possibility to use a new design of swage pin without swage ball employing finite element method. We design three new curved pins, which integrate swage balls in the pin designs. We observe the resulting tightening torque and pin oscillation during swaging process from the finite element simulation. According to the result, we found that the new pin designs can effectively reduce the pin oscillation and increase the tightening torque when comparing to the original pin-ball design. The results from this research will be useful for any further study on the possibility to use pin without ball in the swaging process in the future.**

***Keywords*— Head Gimbal Assemblies (HGAs) / Ball swaging / Finite element method / Tightening torque / Swage pin design**

I. INTRODUCTION

Ball Swaging is the process to attach a complicated tiny piece of HGAs to a suspension arm by shooting a sequence of swage balls, which all have larger diameters than the diameter of the HGA's hole as shown in Figure 1. By shooting swage balls through swage hole, base plates of HGAs are permanently deformed and compressed onto the actuator arm. With the tightening torque occurred on the contact surfaces, base plates are attached to the actuator arm.

In order to validate and compare the quality of new pin designs, the tightening torque values will be compared. The variables that have effect on the tightening torque after the process of ball swaging are:

1) Contact pressure, $P(s)$: happens when the balls compress base plates onto the actuator arm.
2) Friction, μ: happens on the contact surfaces of base plates and actuator arm. The friction value may not be constant depending on the smoothness of the surface.

$$\tau_{Tightening} = \mu r^2 \int_0^{2\pi} \int_0^{l} P(s) ds d\theta, \quad (1)$$

where l is a width of contact area, and 2π is angle of the contact surfaces between base plate and actuator arm. To simplify the integration, we employ trapezoidal rule to perform numerical integration as shown in Figure 2.

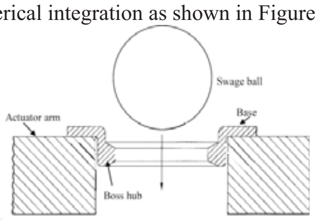

Figure 1 Ball swaging process [4]

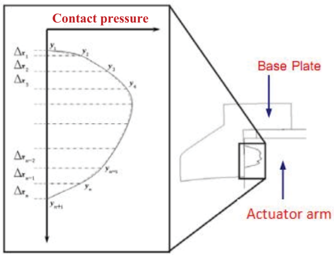

Figure 2 Contact pressure between base plate and actuator arm [2]

The area of each trapezoid can be found as

$$\text{Area} = \frac{1}{2}(y_n + y_{n+1})\Delta x_n, \quad (2)$$

And consider both equations together

[1]Corresponding Author

$$\tau_{tightening} = 2\mu r^2 \pi \sum(\frac{1}{2}(y_n + y_{n+1})\Delta x_n) \quad (3)$$

In the research, the friction coefficient of the base plate and the swage ball is set to be a constant value of 0.3.

II. FINITE ELEMENT MODELING AND MODEL VALIDATION

2.1) Modeling

The 3-D finite element model consists of base plate, actuator arm, top key, slide key, swage pin, swage balls and nozzle. The base plate and actuator arm are created as deformable solids with linear hexahedral elements. The top key and slide key are created as discrete rigid bodies. The swage balls, swage pin and nozzle are created as analytical rigid bodies, as shown in Figure 3

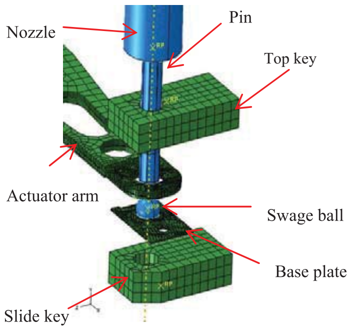

Figure 3 The 3D finite element model for 1-head swaging process

2.2) Load and Boundary conditions

The analysis of swaging process is divided into three main steps; Clamping, Swaging and Unclamping.

1. Clamping step

Loads:

- Clamping load is applied in the vertical direction on the top key.

Boundary conditions:

- The top key is constrained to move only in the vertical direction, and is in contact with the top surface of the actuator arm.
- The slide key is constrained in all directions and rotations, and is in contact with the bottom surface of the base plate.
- The actuator arm's end is fixed.

2. Swaging step

Loads:

- The pin moves with a constant vertical speed. Its impact on the ball causes the ball to move through swage hole. In this experiment three swage balls are used, and the pin is moved three times to shoot three swage balls separately.
- Each swage ball is in contact with the inner hole of the base plate with a coefficient of friction 0.1.

Boundary conditions:

- All boundary conditions are propagated from the previous step.

3. Unclamping step

Loads:

- The clamping load applied on the top key is removed.

Boundary conditions:

- All boundary conditions are propagated from the previous step.

2.3) Analysis Results and validation

By varying the coefficient of friction between base plate and actuator arm, the resulting tightening torque values from the finite element simulation are shown in Table 1. Comparing results to those obtained from the real experiments, the smallest error is about 0.18% where the friction value is set to 0.9, and the modeling method is validated.

TABLE 1
COMPARING TIGHTENING TORQUE OBTAINED FROM EXPERIMENTS AND FE SIMULATION FOR DIFFERENT VALUES OF FRICTION COEFFICIENT.

Friction Coefficient	Tightening torque (N-mm)	Error (%)
0.7	77.768	25.79%
0.8	90.297	13.83%
0.9	104.603	0.18%

Observing the deformation of base plate from finite element simulation, we found that the swage hole after deformation is not in a circular shape as shown in Figure 4, which implies that the deformation is not uniform in all directions. Moreover, the center of swage boss is found to be misaligned from its original position. One possible reason for this is that the guiding pin might oscillate and cause the swage balls to spin during the process. This also affects the contact pressure contour on the contact surfaces of base plate and actuator arm to be non-uniform around the swage hole.

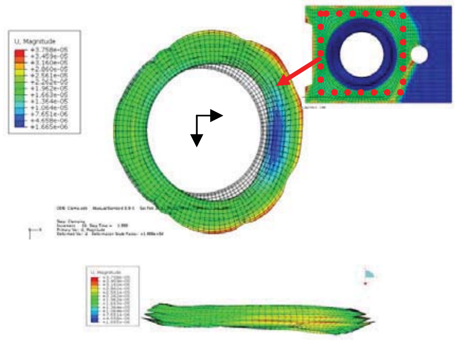

Figure 4 Deformation of swage boss after swaging (scaled x10,000)

III. Finite element modeling and analysis of swaging process without swage ball.

3.1) Modeling, loads and boundary conditions

The original swage pin and balls are replaced with the new pin designs, while all other parts in the model remain the same. In this study, we design three new curved pins, which integrate swage balls together in the pin designs as shown in Figure 5.

1. Cone-shaped pin: Pin diameter changes linearly along the pin axis.
2. Convex-shaped pin: Pin diameter changes rapidly at the beginning and changes gradually when approaching the largest diameter.
3. Concave-shaped pin: Pin diameter changes gradually at the beginning and changes rapidly when approaching the largest diameter.

Cone-shaped pin   Convex-shaped pin   Concave-shaped pin

Figure 5 The new designs of swage pin

3.2) Material properties, loads and boundary conditions

Setting for material properties, loads and boundary conditions remain unchanged

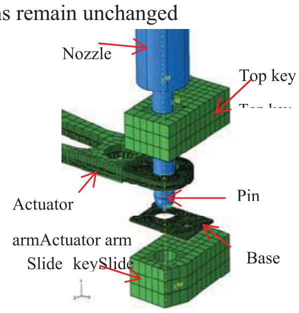

Figure 6 3D model of a set of head and clamping kit

IV. Analysis Results and Discussion

This section compares the finite element results of the original pin-ball design and the new pin designs considering the deformation of base plate, pin oscillations, contact pressure and tightening torque values on the contact surfaces.

4.1) Deformation of base plate

When measuring the deformation of base plate in the radial direction at the position shown in Figure 7, we found that the deformation behaviour of the base plate is corresponding to the pin's shape. The deformation results are plotted in Figure 8. It's clearly shown that the new pin designs tend to deform the base plate more gradually, while the original pin-ball design cause the rapid deformation three times on the base plate.

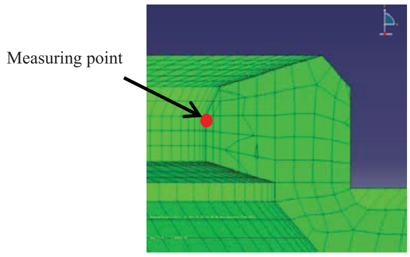

Figure 7 Base plate deformation measuring point

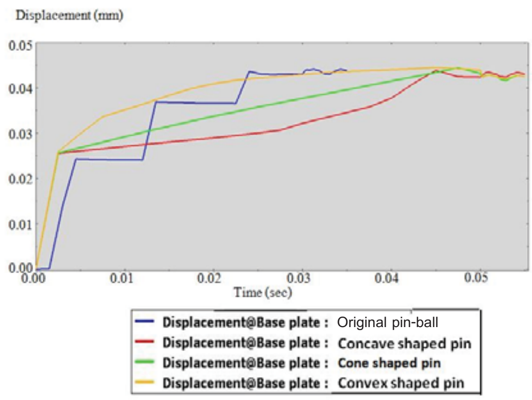

Figure 8 Comparing the displacement of base plate in radial direction for the original pin-ball design and the new pin designs

4.2) Pin and ball oscillation

When comparing the displacement from the swage hole's center line, measuring at pin tips in the new designs, and at the ball centers in the original design, we can see that the new pin designs can successfully reduce the pin and ball oscillation. Figure 9 shows the displacement results. In the original design, the first ball causes the largest displacement, and the value decreases respectively in the two following balls. In the new pin designs, all three designs give lower values of displacement than the original design, however, the concave-shaped pin gives the best result.

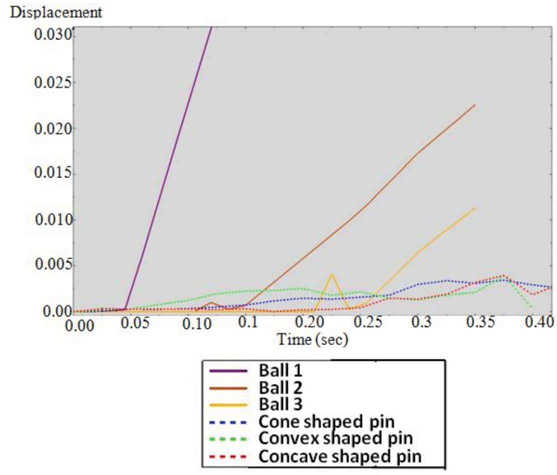

Figure 9 Comparing the displacement from the centreline of the pins and balls in the original design and new pin designs

4.3) Contact pressure

When comparing the contact pressure contour plot, it is clearly shown that the new pin design (Concave-shaped pin) gives a more uniform and wider band of contact pressure than the original pin-ball design.

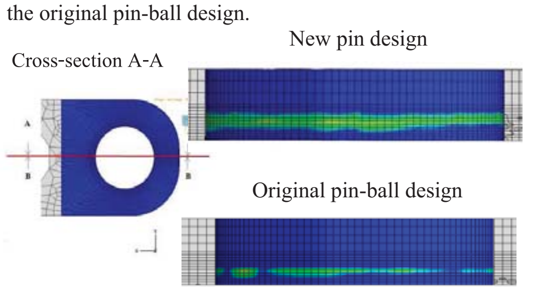

Figure 10 Comparing the contact pressure contour plot of the original design and the new design

4.4) Tightening torque

To measure the swaging quality, tightening torque values are observed and compared. The tightening torque values for the original and new design are shown in Table 2. The results indicate that all of the new pin designs give larger tightening torque values comparing to the original design, and the concave-shaped pin give the best result.

TABLE 2
COMPARING TIGHTENING TORQUE VALUES FOR DIFFERENT PIN DESIGNS

Design	Tightening Torque(N.mm)
Cone-shaped pin	140.873
Convex-shaped pin	121.749
Concave-shaped pin	155.429
Original pin-ball design	104.603

V. CONCLUSIONS

In this research, we study the possibility to use a new design of swage pin without swage ball, employing finite element method. We design three new curved pins, which integrate swage balls to the swage pin including Cone-shaped pin, Convex-shaped pin, and Concave-shaped pin. We observe the deformation of base plate, pin oscillations, contact pressure and tightening torque values on the contact surfaces from the finite element simulation. According to the result, we have found that the new pin designs can effectively reduce the pin oscillation, and increase the contact pressure as well as the tightening torque, comparing to the original pin-ball design. The results from this research will be useful for any further study on the possibility to use pin without ball in the swaging process in the future.

ACKNOWLEDGMENT

We want to express our gratitude to many research assistants at COCARE, FIBO, and Western Digital Thailand, who gave us advices and helps for information and equipments associated in this research to make this research successful.

REFERENCES

[1] K. Aoki and K. Aruga, “Numerical ball swaging analysis of head arm for hard disk drives,” *Microsystem Technologies.*, vol. 13, pp. 943- 949, 2007.

[2] T. Kamnerdtong, S. Chutima and K. Ekintumas, “Effects of Swaging process Parameters on Specimen Deformation,” *8th Asian Symposium on Visualization*, 2005, p. 50.1-50.7.

[3] T. Kamnerdtong, S. Chutima and J. Parirukvijit, “The improvement of deformations and charateristics of HGA during clamping using finite element analysis,” in *Proceedings of the 40th Conference on Winter Simulation*, 2008, p. 1335-1343.

[4] A. Boonseng and S. Chutima, “Study of used swage ball effect on head stack performance,” *KMUTT Research and Development Journal.*, vol.33, pp.207-214, 2010.

[5] S.K. Wadhwa, “Material Compatibility and Some Understanding of the Ball Swaging Process,” *IEEE Transactions on Magnetics.*, vol. 32, pp. 1837 - 1842, May 1996.

[6] F. Jacob, “AL 6061-T6-Elastomer Impact Simulations,” Research Report, Rensselaer Polytechnic Institute, USA, 2005.

[7] *ABAQUS 6.9 Documentation*, Simulia, 2010.

[8] *ASM Metal Handbook*, Volume 18: friction Lubricant and wear technology, P.113.

[9] S. Chutima, T. Kamnerdtong and S. Sangsanon, “Swaging Process Analysis and Improvement of Head Stack Assembly for Hard Disk Drive using Finite Element Method,” *The 23rd Conference of the Mechanical Engineering Network of Thailand*, 2009.

[10] G. R. Johnson and W. H. Cook, “Fracture Characteristics of Three Metals Subjected to Various Strains, Strain rates, Temperatures and Pressures.” *Int. J. Eng. Fract. Mech.*, vol. 21, pp. 31–48, 1985.

[11] T. W. Becker, “On the Effect of Temperature and Strain-rate Dependent Viscosity on Global Mantle Flow, Net Rotation, and Plate-driving Forces,” *Geophysical Journal International*, Vol. 167, pp. 943-957, 2006.